Effect of HIPing on the effective thermal conductivity/diffusivity and the interfacial thermal conductance of uniaxial SiC fibre-reinforced RBSN

H. BHATT, K. Y. DONALDSON, D. P. H. HASSELMAN
Department of Materials Engineering, Virginia Polytechnic Institute and State University, Blacksburg, VA 24061, USA

R. T. BHATT
Ceramics Branch, Materials Division, NASA Lewis Research Center, Cleveland, OH 44135, USA

Hot isostatic pressing (HIPing) was found to increase the thermal diffusivity/conductivity of uniaxial silicon carbide fibre-reinforced reaction-bonded silicon nitride (RBSN) matrix composites, as the result of the densification of the matrix, the increase in the grain size of the silicon carbide and the improved thermal contact between the fibres and the matrix. Transverse to the fibre direction the thermal diffusivity/conductivity was found to be a function of the surrounding gaseous atmosphere due to the access of the gas phase to the fibre–matrix interface, which was facilitated by the existence of an interfacial gap due to the thermal expansion mismatch between the fibres and the matrix. The interfacial conductance was found to exhibit a strong positive temperature dependence as the result of the closure of the interfacial gap with increasing temperature.

1. Introduction

Fibre- or whisker-reinforced ceramic matrix composites offer considerable advantages over single-phase ceramics in applications involving elevated temperatures in view of their improved fracture toughness, non-catastrophic failure mode and lower sensitivity to surface damage. The thermal conduction characteristics of ceramic matrix composites are critical when designing for service conditions involving transient or steady-state heat flow and the possibility of failure by thermal shock and fatigue.

Theoretical studies have shown that the effective thermal conductivity of a. composite depends on the thermal conductivity values, the volume fraction and the distribution of the individual components within the composite [1–6]. Recently, a number of other studies have identified the role an interfacial thermal barrier can play in establishing the effective thermal conductivity of composites [7–10].

For a composite uniaxially reinforced with fibres of circular cross-section, the effective thermal conductivity perpendicular to the fibre axis is [8]

$$K_c = K_m [(K_f/K_m - 1 - K_f/ah_i) V_f$$
$$+ (1 + K_f/K_m + K_f/ah_i)]/[(1 - K_f/K_m$$
$$+ K_f/ah_i) V_f + (1 + K_f/K_m + K_f/ah_i)] \quad (1)$$

where K and V represent the thermal conductivity and volume fraction, respectively, the subscripts c, m, and f

refer to the composite, matrix and fibre phases, respectively, a is the fibre radius and h_i is the interfacial thermal conductance.

The effect of the magnitude of the interfacial conductance on the composite thermal conductivity is governed by its influence on the magnitude of the non-dimensional parameter, K_f/ah_i. For $h_i = \infty$ (i.e. perfect thermal contact) the expression for K_c reverts to the equation derived by Rayleigh [1]. For $h_i = 0$, K_c corresponds to that of a porous composite, and is independent of the value of K_f. Note that for imperfect thermal contact (h_i is finite), the effective thermal conductivity is also a function of the size of the fibres.

Less than perfect thermal contact at the fibre–matrix interface in composites can arise from poor chemical or mechanical adhesion between the fibre and the matrix and from mismatches in their coefficients of thermal expansion. In particular, this latter effect can occur for composites in which the coefficient of thermal expansion of the fibre is greater than that of the matrix. On cooling from the fabrication temperature, internal stresses and interfacial debonding are generated, especially for those composites with poor interfacial adherence. Even with perfect mechanical contact, an interfacial thermal barrier can arise from less than perfect thermal coupling between the dominant mechanism of heat transfer in the individual components of the composite.

For steady-state heat flow parallel to the fibre

direction in a uniaxially reinforced composite, the effective thermal conductivity is not affected by the existence of an interfacial thermal barrier and from the rule of mixtures is given by

$$K_c = K_m[1 - V_f(1 - K_f/K_m)] \qquad (2)$$

Earlier studies on the effect of an interfacial barrier on the effective thermal conductivity concentrated on a silicon carbide fibre-reinforced reaction-bonded silicon nitride matrix composite [11, 12]. The presence of an interfacial gap, which resulted from the thermal expansion mismatch between the fibre and the matrix, was found to play a major role. The presence of such a gap was inferred from the observation that transverse to the fibre direction the effective thermal diffusivity/conductivity was a function of the atmosphere, i.e. it was lower in vacuum than in nitrogen or helium. It was also noted that by the selective oxidation of the interfacial carbon layer, the thermal diffusivity/conductivity of the composite transverse to the fibre direction was lowered even further, with major differences in the values occurring in vacuum, nitrogen or helium.

From the perspective of the present study, it should be noted that the reaction-bonded silicon nitride (RBSN) matrix phase of these earlier studies was relatively porous with a mean value of porosity of about 38%, but with localized regions, especially in the immediate vicinity of the fibres, with pore contents much higher than the average value. Such porosity levels are expected to govern the direct physical contact between the matrix phase and the fibre and thereby affect the value of the interfacial thermal conductance. Removal of the pore phase from the matrix by hot isostatic pressing (HIPing) would modify the thermal contact between the fibre and matrix and thereby affect the overall effective thermal conductivity of the composite. The purpose of the present paper is to report the results of such a study.

2. Experimental procedure
2.1. Material
The starting materials for the composites of this study were double-coated SCS-6 SiC monofilaments and high-purity silicon powder having an average particle size of 0.3 μm. The SiC fibres, produced by chemical vapour deposition of methyltrichlorosilane on to a heated carbon substrate, have a complex microstructure and can be regarded as microcomposites in themselves. A schematic diagram of the cross-section of the fibre is shown in Fig. 1a. The fibre consists essentially of an SiC sheath with an outer diameter of 142 μm surrounding a pyrolytic graphite-coated carbon core with diameter of 37 μm. The sheath consists entirely of columnar β-SiC grains and contains two zones; the inner zone, referred to as A in Fig. 1a, contains carbon-rich SiC and the outer zone, referred to as B, is essentially stoichiometric SiC. The outer surface of the SiC sheath contains two layers of a carbon-rich coating, for which the chemical composition as a function of thickness is shown schematically in Fig. 1b.

The composites were fabricated by a three-step
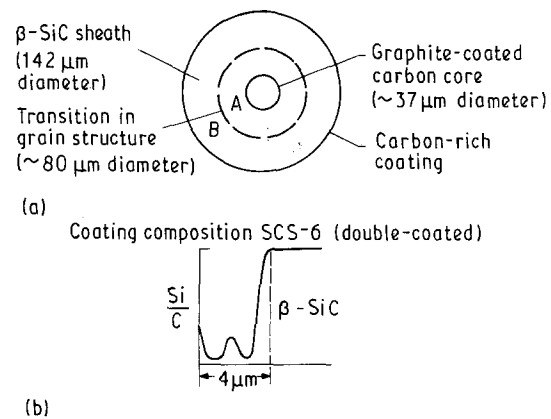
Figure 1 Schematic drawing of an SiC fibre: (a) cross-section and (b) composition profile of carbon coating.

process. In the first step, SiC fibre mats and silicon cloth were consolidated using two different polymer fugitive binders – one polymer for maintaining proper spacing between the fibres in the fibre mat, and the other polymer for preparing pliable silicon cloth. The volume fraction of fibres in the final composite was controlled by either varying the thickness of the silicon cloth or by changing the spacing between fibres in the mat. In the second step, alternate layers of SiC fibre mats and silicon cloth were stacked in a metal die and pressed in a vacuum hot press under an applied stress ranging from 27–200 MPa for up to 1 h in the temperature range 600–1000 °C. In the third step, the consolidated SiC/Si preforms were heat treated in a high-purity (≈ 99.99%) nitrogen environment at temperatures ranging from 1000–1400 °C for up to 100 h to convert them to the their final form. The typical dimensions of the as-nitrided composite panels were 150 mm × 50 mm × 2.2 mm. Some of the as-nitrided SiC/RBSN composites were further densified by HIPing in an argon atmosphere at a pressure of 138 MPa and a temperature of 1850 °C for a period of 1 h. The density of the as-nitrided composite was found to be 2.17 g cm^{-3}, whereas the density of the HIPed composite was measured to be 3.05 g cm^{-3}.

Fig. 2a and b show representative photomicrographs of polished cross-sections of as-nitrided and HIPed composite specimens, respectively. The fibre volume fraction was approximately 28% in the as-nitrided composite and 42 vol% in the HIPed composite. The matrix phase of the as-nitrided composite contained about 38% porosity, whereas in the HIPed composite the matrix phase was essentially pore-free. The carbon core, the surface coating and the two silicon carbide zones in the fibres are clearly evident.

Fig. 3a and b show scanning electron micrographs of the regions in the immediate vicinity of a fibre in an as-nitrided and HIPed composite, respectively. In the as-nitrided composite the highly porous regions in the matrix phase immediately adjacent to the fibre are clearly evident. In the HIPed composite, this region is absent.

For purposes of comparison, samples were also made of the as-nitrided and HIPed RBSN matrix without fibres, following identical fabrication techniques used for preparation of the composite samples.
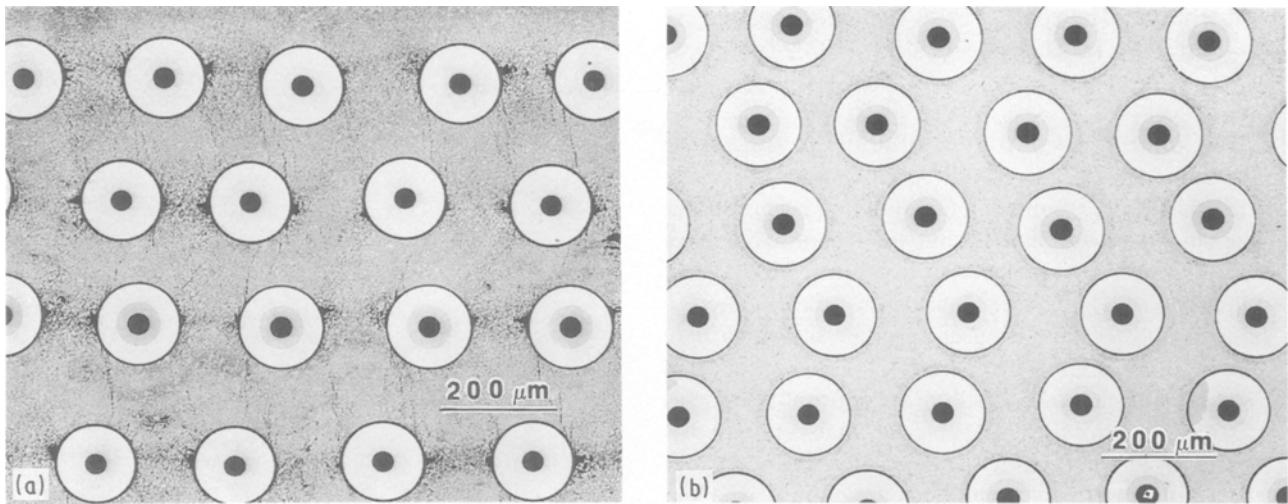
Figure 2 Optical micrograph of a cross-section of uniaxially SiC fibre-reinforced reaction-bonded silicon nitride transverse to the fibre direction (a) as-nitrided and (b) HIPed.
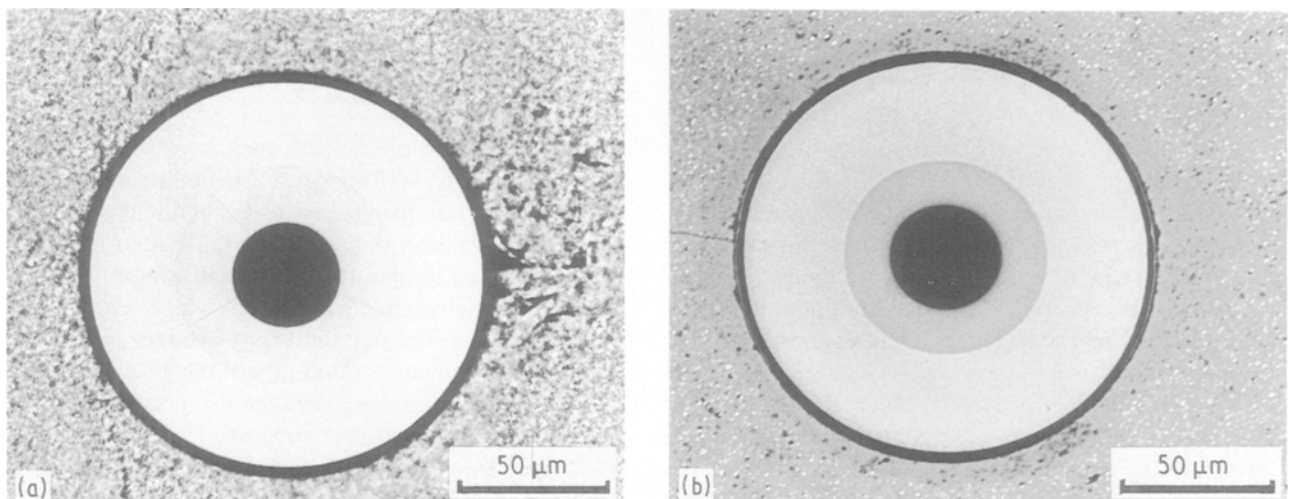
Figure 3 Scanning electron micrograph of polished section in the immediate vicinity of a fibre: (a) as-nitrided and (b) HIPed.

2.2. Determination of thermophysical properties

The effective thermal diffusivity was measured by the laser-flash technique [13, 14]. The specimens, in the form of square platelets with dimensions of approximately 8 mm × 8 mm × 2 mm, were cut from the larger as-nitrided and HIPed blocks. A glass-neodymium laser was used as the flash source. The specimens were lightly coated with colloidal carbon to promote absorption and prevent direct transmission of the laser pulse. An InSb infrared detector was used to monitor the transient temperature rise of the specimen up to temperatures of 700 °C and a silicon photodiode detector was used for temperatures above 700 °C. The detectors viewed a circular area having a diameter of ~ 5 mm. The thermal diffusivity up to 1000 °C was measured at intervals of about 100 °C in helium and nitrogen at atmospheric pressure and in vacuum at a pressure of about 0.13 Pa.

The specific heat was measured by differential scanning calorimetry from room temperature to 600 °C using sapphire as the standard. Data from 600–1000 °C were obtained by extrapolation guided by general trends presented in the literature.

The values for the thermal conductivity were calculated by multiplying the data for the thermal diffusivity with the product of the density and the specific heat. In this manner, values for the thermal conductivity were established from room temperature to 1000 °C for the as-nitrided and HIPed matrix phase and for the composites parallel and perpendicular to the fibre direction.

The coefficients of linear thermal expansion for the matrix and composites perpendicular to the fibre direction were found to be equal, with a mean value of 3.0 × 10^{-6} °C^{-1} over the range from room temperature to 1200 °C. For the composite parallel to the fibre direction, the corresponding value for the coefficient of thermal expansion was 3.6 × 10^{-6} °C^{-1}. These values were used during the calculation of the thermal diffusivity to adjust for the increase in sample dimension with increasing temperature. These values were also used in the calculation of the thermal conductivity to adjust for the decrease in density with increasing

temperature. The coefficient of thermal expansion of the fibres was measured to be $4.53 \times 10^{-6}\,°C^{-1}$.

2.3. Calculation of the interfacial conductance

The value for the interfacial conductance was calculated based on a number of simplifying assumptions. The silicon nitride matrix and the silicon carbide of the fibres were assumed to exhibit isotropic thermal conductivity. The fibres themselves were considered to be a composite consisting of an outer silicon carbide sheath and a carbon inner core. This carbon core, in view of its preferred crystallographic orientation, was assumed to exhibit anisotropic thermal conductivity. The thermal conductivity of the silicon carbide phase in the fibres parallel to the fibre direction was calculated from the thermal conductivity of the matrix, the thermal conductivity of the composite for heat flow parallel to the fibre direction and the thermal conductivity of the core using the rule of mixtures for a three-phase composite. The thermal conductivity of the carbon core was inferred from the correlation between Young's modulus and the thermal conductivity established by Nysten et al. [15]. For a value of Young's modulus for the carbon core of 41 GPa [16], this led to a value of the thermal conductivity of the carbon core parallel to its axis of $29\,W\,m^{-1}\,K^{-1}$. This low value for the thermal conductivity, which is well below the value for many other carbon fibres, indicates that the crystal structure of the fibre core is highly defective. For this reason, the thermal conductivity of the core was assumed to be independent of temperature as the phonon mean-free-path was thought to be primarily governed by the defect structure. It should be noted that this assumption introduces little error in the final results of the thermal conductivity of the fibres as the core represents only 6.8% volume fraction of the fibre and an even smaller value of the composite as a whole. The transverse thermal conductivity of the silicon carbide in the fibres was assumed equal to the thermal conductivity of the fibres parallel to their axis. The carbon core within the fibres, in view of its highly preferred crystallographic orientation, is expected to exhibit highly anisotropic thermal conductivity [17–19]. For this reason, transverse to the core the thermal conductivity is expected to be quite low compared to the value parallel to the core and for simplicity was assumed to be zero. Again, as pointed out earlier, this assumption is not expected to introduce a major error, as the core represents a small volume fraction of the fibres or composite as a whole. The effective thermal conductivity of the fibres transverse to their axis was then obtained using the appropriate porosity correction from Equation 1. From the resulting thermal conductivity data for the matrix, fibres and the composite sample with heat flow transverse to the fibre direction, the interfacial thermal conductance was then calculated by means of Equation 1.

3. Results, discussion and conclusions

Fig. 4 shows the experimental data for the thermal diffusivity of the as-nitrided and HIPed RBSN matrix
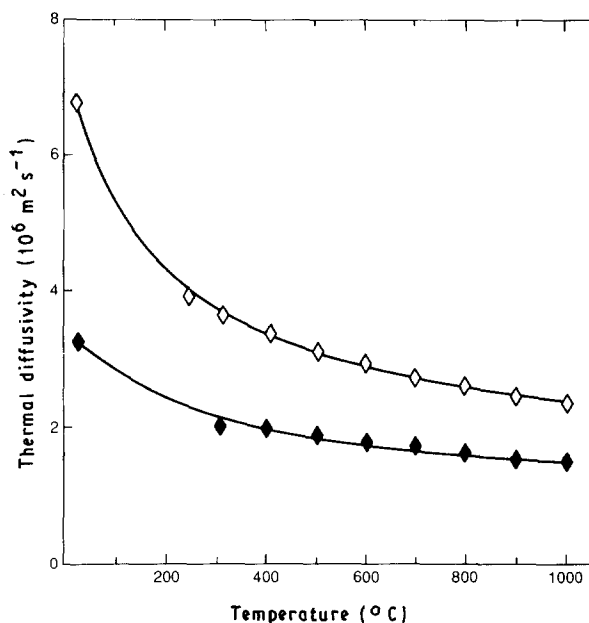
Figure 4 Thermal diffusivity of (♦) as-nitrided and (◇) HIPed reaction-bonded silicon nitride matrix phases in helium, nitrogen and vacuum.

phases in atmospheres of helium, nitrogen and vacuum. Clearly, HIPing caused a significant increase in the thermal diffusivity due to the elimination of the pore phase. Within the experimental scatter and possible specimen-to-specimen variation, the differences in gaseous environments appeared to have no significant effect on the thermal diffusivity of either matrix. In fact, the experimental data in the three gaseous atmospheres were so close, they could not be plotted separately. The relative temperature dependence of the data, shown in Fig. 4, is typical for dielectric materials in which phonon heat transfer is the primary mechanism of heat conduction.

Fig. 5 shows the data for the thermal diffusivity of as-nitrided and HIPed composite samples for heat
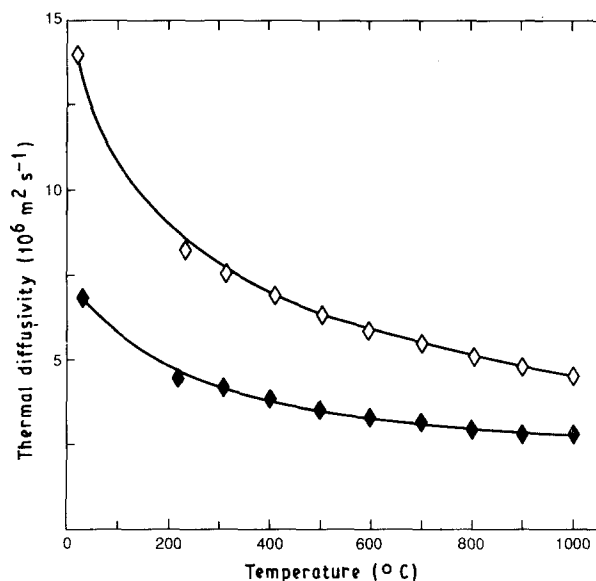
Figure 5 Thermal diffusivity of (♦) as-nitrided and (◇) HIPed SiC fibre-reinforced reaction-bonded silicon nitride parallel to the fibre direction in helium, nitrogen and vacuum.

flow parallel to the fibre direction in the presence of helium, nitrogen and vacuum atmospheres. Again, HIPing caused a significant increase in the thermal diffusivity, attributable to the densification of the matrix and, as to be discussed, an increase in the thermal conductivity of the fibres.

Comparison of Figs 4 and 5 shows that the presence of the fibres increases the effective thermal diffusivity by about a factor of two over the corresponding value for the matrix. This implies that the thermal conductivity of the fibres significantly exceeds the value for the matrix. These values will be presented shortly.

Fig. 6 shows the data for the effective thermal diffusivity of as-nitrided and HIPed composite samples transverse to the fibre direction in helium, nitrogen and vacuum. As expected, HIPing increased the thermal diffusivity for all environmental conditions. Also note that the thermal diffusivity for the as-nitrided and HIPed samples in the different atmospheres exhibits significant differences. This observation came as quite a surprise, at least to these authors. In order to find a plausible explanation for this effect it should be noted that the coefficient of thermal expansion of the silicon carbide fibre is higher than that for the matrix. This implies that on cooling from the nitriding temperature, tensile internal stresses are generated across the interface, which, for weakly bonded interfaces, can lead to interfacial cracking. Assuming that such cracks are uniform around the interface, their width at room temperature is of the order of 0.1 µm, as calculated from the differences in the coefficients of thermal expansion of the fibre and the matrix, the fibre size and the range of temperature over which the composite is cooled. Such a crack width is sufficient for the environmental atmosphere to enter the interface and contribute to the conduction
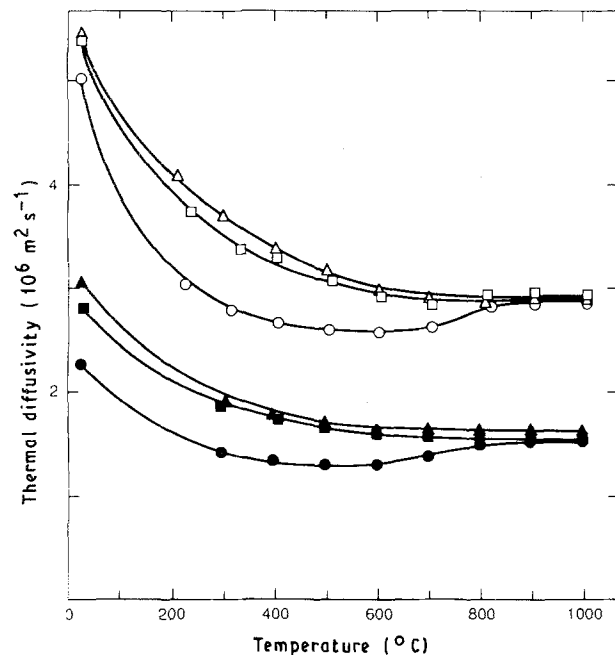
of heat across the interface. Raising the temperature of the sample will result in a decrease in the width of the interfacial crack. This, in turn, will result in improved direct physical contact and expulsion of the gas phase from the interface as the temperature approaches the composite's processing temperature. This is in agreement with the observation that the thermal diffusivity data in vacuum are well below the corresponding values in helium and nitrogen at the lower temperatures, but are almost equal at temperatures from about 800–1000 °C. Direct evidence for the existence of such a crack by scanning electron microscopy of fracture surfaces could not be obtained. However, parallel studies of mechanical behaviour showed that interfacial fracture usually occurred within the carbon coating on the SiC fibres and occasionally at the interface between the SiC and the carbon layer, but not at the interface between the carbon coating and the silicon nitride. Of course, the effect of the gas phase on the thermal diffusivity represents indirect evidence for the existence of an interfacial gap.

The above unexpected finding suggests that for the as-nitrided and/or HIPed composites the thermal expansion crack is expected to play a major role in establishing the effective thermal conductivity transverse to the fibre direction. Fig. 6 also indicates that for any given processing history, the values of the thermal diffusivity are highest in a helium atmosphere, followed by nitrogen and are the lowest in vacuum. This ranking is in accordance with the ranking of the thermal conductivity of helium, nitrogen and vacuum, providing indirect evidence for the hypothesis that the

Figure 6 Thermal diffusivity of (▲, ■, ●) as-nitrided and (△, □, ○) HIPed SiC fibre-reinforced reaction-bonded silicon nitride transverse to the fibre direction in (△, ▲) helium, (□, ■) nitrogen and (○, ●) vacuum.
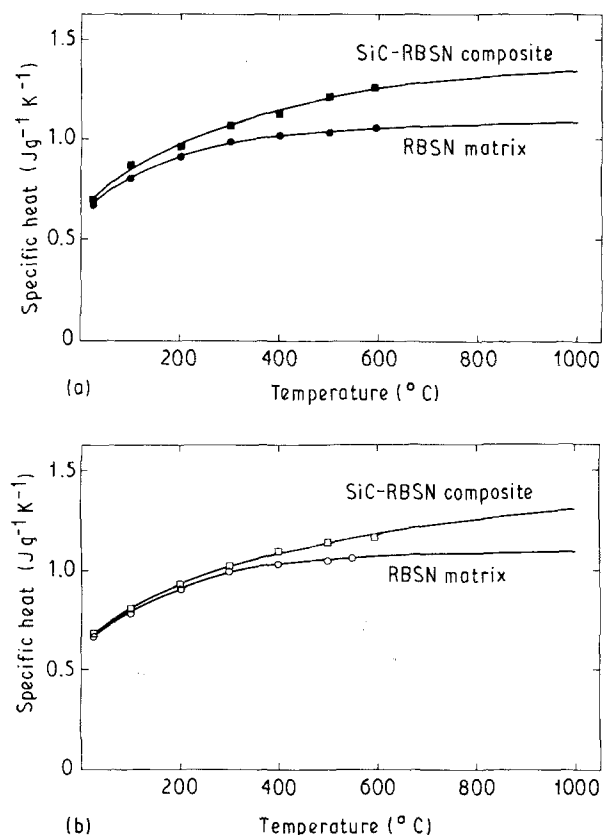
Figure 7 Experimental and extrapolated data for the specific heat (a) as-nitrided and (b) HIPed, SiC fibre-reinforced silicon nitride.

gaseous atmosphere can enter the interfacial gap and thereby contribute to the heat transfer between the fibre and matrix. A more detailed discussion of the nature of the heat transfer across gaps will be presented as part of the discussion of the values for the interfacial thermal conductance.

Fig 7a and b show the experimental and extrapolated values for the specific heat of the as-nitrided and HIPed RBSN matrix and the silicon carbide–silicon nitride composite, respectively. The magnitude of the specific heat for the matrix phase appears to be unaffected by the HIPing process within the accuracy of the experimental method, estimated to be about 3%. The HIPing, however, appears to have decreased the specific heat of the composite samples. No information is available to explain this effect.

Fig. 8 shows the calculated values for the thermal conductivity of the as-nitrided and HIPed RBSN matrix samples in helium, nitrogen and vacuum. These data reflect the same relative differences as those found for the thermal diffusivity, with the exception that because of the positive temperature dependence of the specific heat, the temperature dependence of the thermal conductivity is less negative than for the thermal diffusivity.

Fig. 9 shows the calculated values for the thermal conductivity of the composite samples for heat flow parallel to the fibre direction. Again, these data show the same relative values as found for the thermal diffusivity, with the same exception, that the relative temperature dependence of the thermal diffusivity is more negative than the corresponding dependence of the thermal conductivity. The data of Fig. 9 also indicate that HIPing appears to have increased the relative negative temperature dependence of the thermal conductivity compared to the as-nitrided composite. Calculation of the fibre thermal conductivity
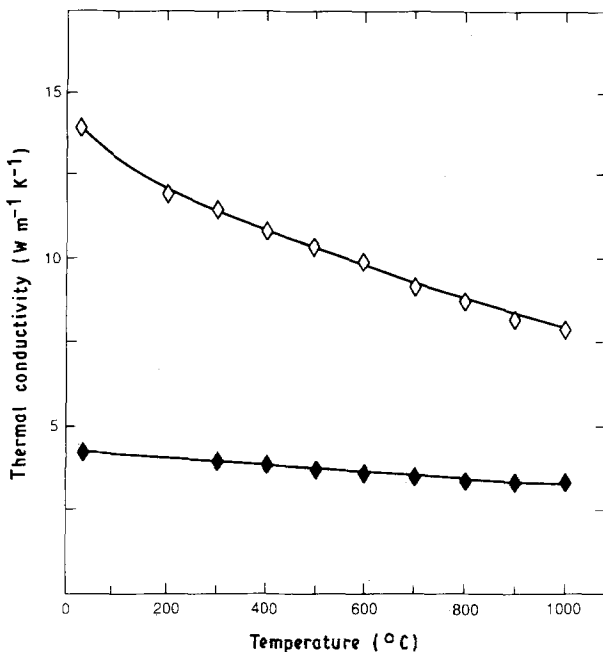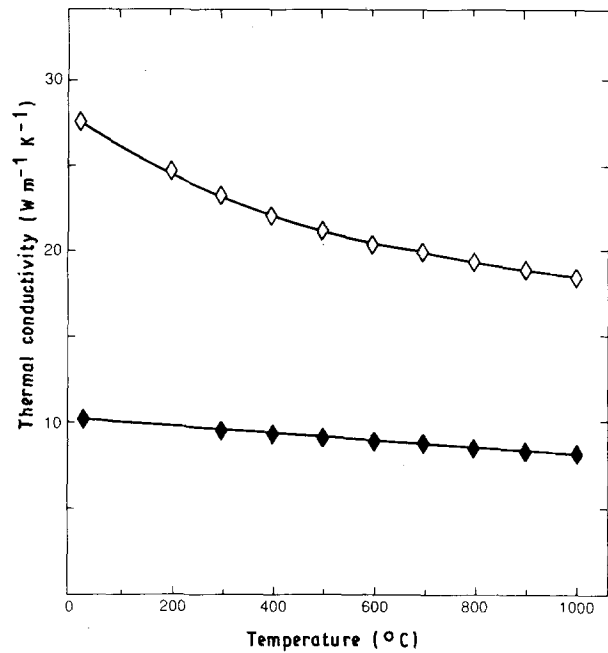
Figure 9 Calculated values for the thermal conductivity of (◆) as-nitrided and (◇) HIPed SiC fibre-reinforced reaction-bonded silicon nitride parallel to the fibre direction in helium, nitrogen and vacuum.

from the thermal conductivity data of the matrix and the composite for heat flow parallel to the fibre direction, using Equation 2, showed that HIPing also increased the thermal conductivity of the fibres significantly. Such an increase most likely is the result of the annealing of structural defects, introduced in the silicon carbide during chemical vapour deposition, and grain growth at the much higher temperature of the HIPing process. As a result, the temperature dependence of the thermal conductivity of the HIPed silicon carbide fibres is expected to be more controlled by the negative temperature dependence due to phonon–phonon interactions, rather than the athermal effects associated with phonon–defect interactions. In turn, this is reflected in the relative temperature dependence of the composite samples.

Fig. 10 shows the calculated values for the thermal conductivity of the as-nitrided and HIPed composite samples for heat transfer transverse to the fibre direction in helium, nitrogen and vacuum. These data reflect the relative differences in the data for the thermal diffusivity shown in Fig. 6, with the exception that the relative temperature dependence of the thermal conductivity is less negative than the corresponding dependence for the thermal diffusivity, for the same reason stated earlier.

Fig. 11 shows the values for the thermal conductivity of the fibres parallel and transverse to the fibre direction, calculated in the manner described earlier. The thermal conductivity transverse to the fibre direction is lower than the corresponding value parallel to the fibre direction, because the contribution of the carbon core (with thermal conductivity assumed to be equal to zero) will be relatively greater transverse to the fibre direction than in the parallel direction. This is easily ascertained by a comparison of Equation 1

Figure 8 Calculated values for the thermal conductivity of the (◆) as-nitrided and (◇) HIPed silicon nitride matrix in helium, nitrogen and vacuum.
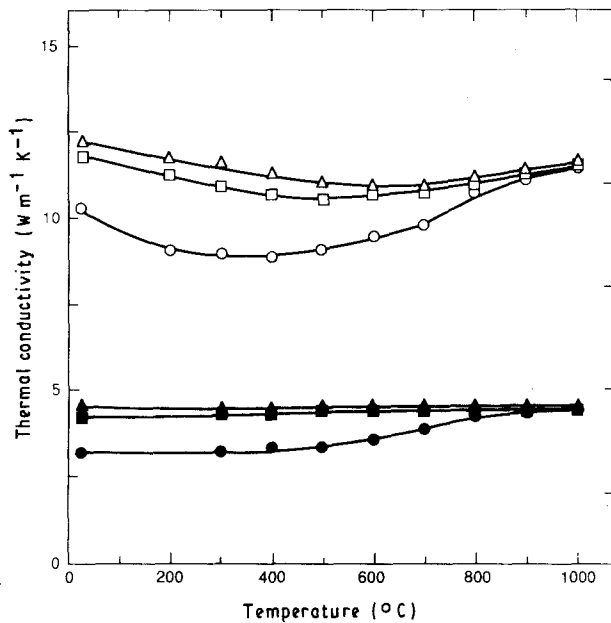
Figure 10 Calculated values for the thermal conductivity of ($\blacktriangle$, $\blacksquare$, $\bullet$) as-nitrided and ($\triangle$, $\square$, $\bigcirc$) HIPed SiC fibre-reinforced reaction-bonded silicon nitride transverse to the fibre direction in ($\triangle$, $\blacktriangle$) helium, ($\square$, $\blacksquare$) nitrogen and ($\bigcirc$, $\bullet$) vacuum.
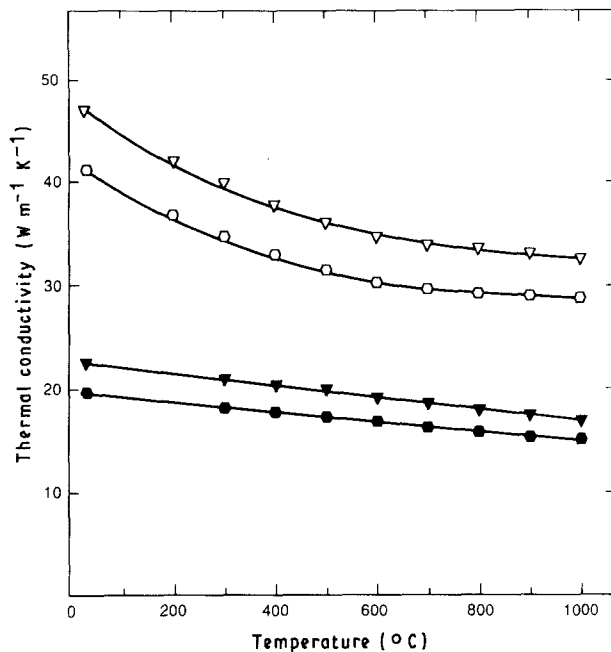
Figure 11 Calculated values for the ($\triangledown$, $\blacktriangledown$) longitudinal and ($\bigcirc$, $\spadesuit$) transverse thermal conductivity of SiC fibres ($\blacktriangledown$, $\spadesuit$) prior to and ($\triangledown$, $\bigcirc$) following HIPing in helium, nitrogen and vacuum.

(with $h_i = 0$) and Equation 2. The transverse conductivity is lower than the parallel conductivity by about 13%. The data of Fig. 11 also indicate that the HIPing operation has led to a significant increase of the thermal conductivity of the fibres, of as much as a factor of 2 at room temperature. Transmission electron microscopy showed that this increase can be attributed to the extensive growth of crystallites, rather than to a decrease in density of the stacking faults. The data also confirm the earlier speculation that the relative negative temperature dependence of the thermal conductivity of the SiC fibres in the HIPed

composite is greater than in the as-nitrided composite, which represents evidence for a decrease in the density of lattice defects, such as vacancies. Nevertheless, whether in the as-nitrided or HIPed composites, the magnitude of the thermal conductivity of the SiC fibres is still relatively low, compared to sintered SiC with values at room temperature near $100\ \mathrm{W\,m^{-1}\,K^{-1}}$, BeO-doped SiC with a value near $200\ \mathrm{W\,m^{-1}\,K^{-1}}$ or a high-purity single crystal with a value approaching $500\ \mathrm{W\,m^{-1}\,K^{-1}}$ [20, 21]. Some of the differences in the data shown in Fig. 11 also reflect the differences in the experimental thermal diffusivity values, possibly related to transverse transient heat flow, as discussed earlier.

Fig. 12 shows the values for the interfacial thermal conductance, calculated, using Equation 1, from the data for the thermal conductivity of the matrix, fibres and the composite for heat flow transverse to the fibre direction. For simplicity, the pore phase in the immediate vicinity of the fibre was assumed to be part of the interfacial conductance, so that the calculation of the conductance could be based on the value of the conductivity of the homogeneous matrix.

In comparing the data of Fig. 12, it should be noted that the interfacial conductance is the sum of the conductances due to heat transfer as the result of direct physical contact across the interface, heat transfer by gaseous conduction and heat transfer by radiation at those positions where no direct contact across the interface exists, expressed by [22]

$$h_i = h_c + h_g + h_r \tag{3}$$
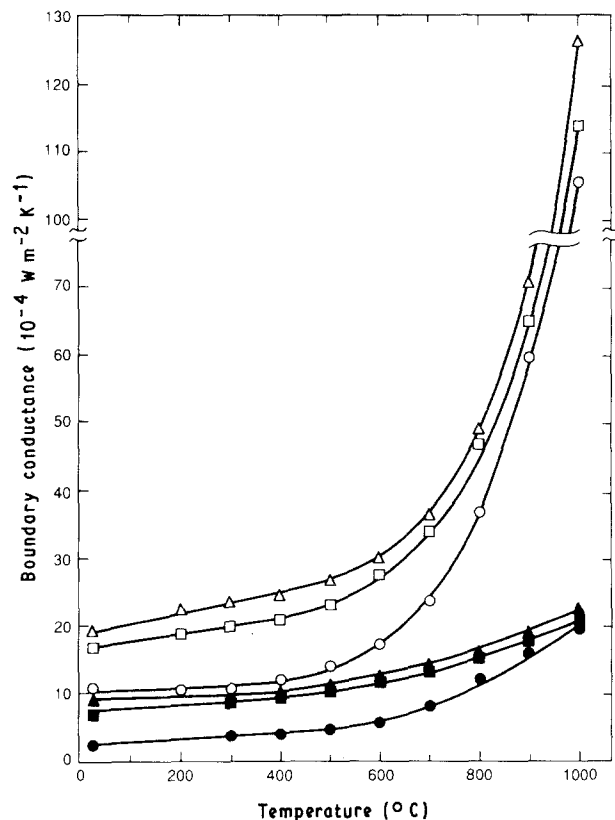
Figure 12 Calculated values for the interfacial conductances in ($\blacktriangle$, $\blacksquare$, $\bullet$) as-nitrided and ($\triangle$, $\square$, $\bigcirc$) HIPed SiC fibre-reinforced silicon nitride composites for heat flow transverse to the fibre direction in ($\triangle$, $\blacktriangle$) helium, ($\square$, $\blacksquare$) nitrogen and ($\bigcirc$, $\bullet$) vacuum.

where h_c, h_g and h_r are the contact, gaseous and radiative conductances, respectively.

The radiative conductance can be derived to be [11]

$$h_r = [4\varepsilon/(2 - \varepsilon)]\sigma n T^3 \qquad (4)$$

where ε is the emissivity of the two surfaces (assumed to be equal), σ is the Stefan–Boltzmann constant, n is the refractive index of the medium within the gap and T is the absolute temperature. Substitution of reasonable values for ε and n into Equation 4 indicates that over the temperature range of this study the radiative conductance is negligible compared to the magnitude of the values shown in Fig. 12.

The contact conductance, h_c, is a strong function of the roughness of the two surfaces in contact and is expected to vary from one situation to another [23]. Because the degree of contact between the fibres and matrix of the composites of this study is not easily established, no independent estimate of the contact conductance can be made. Furthermore, as gaseous conduction will occur only at those interfacial regions with no direct physical contact, the processes of contact and gaseous interfacial conduction are expected to be competitive.

The gaseous conductance, h_g, is a function of the ratio of the mean free path, $\bar{l}$, of the gaseous species and the width, d, of the interfacial gap, defined by the Knudsen number

$$N_{Kn} = \bar{l}/d \qquad (5)$$

For $N_{Kn} \ll 1$, referred to as the "continuum regime", the gaseous heat transfer is controlled by the collisions between the gaseous species. In this regime, the gaseous conductance is

$$h_g = K/d \qquad (6)$$

where K is the thermal conductivity of the gas. In the continuum regime, h_g is independent of pressure and inversely proportional to the gap thickness.

For $N_{Kn} > 10$, inter-atomic or inter-molecular collisions are rare and the conductance is controlled by the energy exchange during the collisions of the gaseous species with the surfaces of the gap. In this regime, referred to as the "molecular regime", the conductance is given by [23]

$$h_g = (c_p\mu/\bar{l})[(\gamma + 1)/2\gamma][(2 - C_1)/C_1$$
$$+ (2 - C_2)/C_2]^{-1} \qquad (7)$$

where c_p and μ are the specific heat and viscosity of the gas phase, C_1 and C_2 are the thermal accommodation coefficients for each surface, γ is the ratio of the specific heats at constant pressure and constant volume and $\bar{l}$ is the mean free path of the gas. The thermal accommodation coefficient represents the efficiency of energy exchange during the collision between the gap surfaces and the gaseous atomic or molecular species.

In the molecular regime, the gaseous conductance, h_g, as expressed by Equation 6, is independent of the gap thickness and is directly proportional to pressure. For the mean gap thickness for the present samples of the order of 0.1 μm, and values for the mean free path at the pressures of this study [24, 25], the gaseous

conductance is expected to be governed by criteria for the molecular regime.

Because no quantitative information is available on any measure of direct physical contact across the interface or on the magnitude of the thermal accommodation coefficients, independent quantitative estimates of the contact and gaseous conductances cannot be given at this time. For this reason, when discussing the data shown in Fig. 12, emphasis will be placed on a comparison of the data. It is of interest to note, however, that the conductance values shown in Fig. 12 compare favourably with those found in experimental studies of surfaces in contact [26, 27].

The data of Fig. 12 indicate that the nature of the gaseous phase has a significant effect on the magnitude of the interfacial conductance. Because of the almost complete absence of a gaseous phase under vacuum conditions, it appears reasonable to conclude that the conductance in vacuum represents the contact conductance due to direct physical contact across the interface. The difference between the conductance values in vacuum and the total conductance in helium or nitrogen must be attributed to the contribution of the gaseous conductance. The relative values of the conductances in helium and nitrogen are in accordance with the differences in the mean velocity of the helium atoms and the nitrogen atoms, inferred from the kinetic theory of gases. It should be noted that the actual values for the accommodation coefficients for helium and nitrogen could well differ significantly, so that no quantitative measure of the relative differences in the gaseous conductances for helium and nitrogen can be made at this time.

Of particular interest is the finding, as seen in Fig. 12, that the conductance values for the as-nitrided and HIPed samples increase with temperature. As discussed earlier, most likely this effect can be attributed to the closure of the thermal expansion crack, due to the thermal expansion mismatch between the fibre and matrix, as the composite is heated again towards the temperature at which it was fabricated. Related to this effect is the finding that the relative difference between the conductances in vacuum and helium or nitrogen decreases with increasing temperature. This is expected, as with increasing temperature and associated tendency for crack closure, increased physical contact will occur between the fibre and matrix with a corresponding decrease in the opportunity for gaseous heat transfer. The conclusion that the strong positive temperature dependence of the conductance is the result of increased physical contact across the interfacial thermal expansion crack is supported by the findings, to be published elsewhere, that the interfacial shear stress required to cause sliding between the fibre and matrix also increases with temperature.

The HIPing operation caused a significant increase in the magnitude as well as the temperature dependence of the conductance. A number of reasons, necessarily qualitative, can be given for this effect. The primary effect of the HIPing operation was the densification of the matrix. As a result, for the as-made composites following HIPing, the fibre is in far greater

degree of direct physical contact with the matrix than was the case for the highly porous matrix in the as-nitrided material. For the porous matrix much of the heat transfer between the fibre and matrix would require gaseous conduction through the pores at the fibre–matrix interface. This contribution, however, is expected to be minor, as, in general, the effective thermal conductivity of a gas phase in a pore, whether in the molecular or continuum regime, is much less than the net thermal conductivity of the direct solid-to-solid contact. As a very first approximation, a pore phase will reduce the relative area of direct physical contact at the fibre–matrix interface by an amount equal to the volume fraction porosity. With a pore phase content of approximately 37% for the matrix phase of the as-nitrided composite, elimination of the pore phase would cause an increase in the area of direct interfacial contact by about 50%. This estimate, however, assumes that for the porous matrix, perfect contact exists between the solid fraction of the matrix and the fibres. In other words, it assumes that the morphology of the solid part of the matrix conforms exactly to the morphology of the fibre surface. The nitriding reaction, however, was not carried out at a pressure at which the matrix could be compacted against the fibre. Therefore, any direct physical contact between the fibre and matrix most likely occurs at the outer points or edges of the individual grains of the matrix. If so, the fractional area of direct interfacial contact is expected to be a great deal less than the volume fraction of solid within the matrix phase. HIPing, however, will deform the grains to greatly increase the direct contact between the fibre and matrix with a corresponding large increase in the interfacial conductance. It was hoped that evidence in the form of fractographs could be presented which would support this hypothesis. Unfortunately, for the as-nitrided and HIPed composite samples, fracture always occurred at the interface between the silicon carbide and the carbon coating or within the carbon coating rather than at the carbon–silicon nitride inter-face. Looking at this from another angle, the overall interfacial thermal conductances represent the sum effects of the silicon carbide–carbon interface, the carbon–matrix interface and possible effects within the carbon coating itself. The HIPing operation is expected to have primarily affected the conductance of the matrix–carbon coating interface.

In general, the observations of this study indicate the very powerful role interfaces can play in the effective thermal conductivity of composites. Especially seen in the light of the current technical development of tailoring interfaces with fibre coatings in order to optimize interfacial mechanical properties and corresponding fracture toughness of composites, significant interfacial thermal effects should be expected and accounted for.

The results of this paper also clearly indicate that the measurement of the thermal diffusivity or conductivity can be used as a qualitative non-destructive tool to determine the integrity of the fibre–matrix interface and to monitor microstructural changes occurring in the fibres, matrix and interface during fabrication or during service.

References

1. LORD RAYLEIGH, *Phil. Mag.* **34** (1892) 481.
2. J. C. MAXWELL, "A Treatise on Electricity and Magnetism", 3rd Edn (Oxford University Press, 1904).
3. D. A. G. BRUGGEMAN, *Ann. Physik* **24** (1935) 636.
4. R. E. DE LA RUE and C. W. TOBIAS, *J. Electrochem. Soc.* **106** (1959) 827.
5. Z. HASHIN, *J. Compos. Mater.* **2** (1968) 284.
6. S. C. CHENG and R. I. VACHON, *Int. J. Heat Mass Transfer* **12** (1969) 249.
7. H. HATTA and M. TAYA, *J. Appl. Phys.* **59** (1986) 1851.
8. D. P. H. HASSELMAN and L. F. JOHNSON, *J. Compos. Mater.* **21** (1987) 508.
9. Y. BENVENISTE, *J. Appl. Phys.* **61** (1987) 2840.
10. Y. C. CHIEW and E. G. GLANDT, *Chem. Engng Sci.* **42** (1987) 2677.
11. H. BHATT, K. Y. DONALDSON, D. P. H. HASSELMAN and R. T. BHATT, *J. Amer. Ceram. Soc.* **73** (1990) 312.
12. *Idem.*, in "Thermal Conductivity 21", edited by C. J. Cremers and H. A. Fine (Plenum Press, New York, 1990) pp. 597–609.
13. W. J. PARKER, R. J. JENKINS, C. P. BUTLER and G. L. ABBOTT, *J. Appl. Phys.* **32** (1961) 1679.
14. R. C. HECKMAN, *ibid.* **44** (1973) 1455.
15. B. NYSTEN, L. PIREAUX and J. P. ISSI, in "Thermal Conductivity 19", edited by D. W. Yarbrough (Plenum Press, New York, NY, 1988) pp. 341–50.
16. J. A. McKEE and L. A. JOO, in "Proceedings of the 3rd International Conference on CVD", edited by F. A. Gloski (American Nuclear Society, Hinsdale, IL, 1972) pp. 536–51.
17. S. NASU, T. TAKAHASHI and T. KIKUCHI, *J. Nucl. Mater.* **43** (1972) 72.
18. T. TANAKA and H. SUZUKI, *Carbon* **10** (1972) 253.
19. M. R. NULL, W. W. LOZIER and A. W. MOORE, *ibid.* **11** (1973) 81.
20. D. P. H. HASSELMAN, in "Thermal Conductivity 20", edited by D. P. H. Hasselman and J. R. Thomas Jr (Plenum Press, New York, 1989) pp 141–53.
21. G. A. SLACK, *J. Appl. Phys.* **35** (1964) 3460.
22. W. P. LEUNG, A. C. TAM, *ibid.* **63** (1988) 4505.
23. G. S. SPRINGER, in "Advances in Heat Transfer", Vol. 7, edited by T. F. Irvine and J. P. Hartnett (Academic Press, New York, 1971) pp. 163–218.
24. F. W. SEARS, "Introduction to Thermodynamics" (Addison-Wesley Cambridge, MA, 1955).
25. "Handbook of Chemistry and Physics", 66th Edn, edited by R. C. Weast, M. J. Astle and W. H. Beyer (CRC Press, Boca Raton, FL, 1985–86).
26. T. F. LEMCZYK and M. M. YOVANOVICH, *Heat Transfer Engng* **8** (1987) 35.
27. C. V. MADHUSUDANA and A. V. LITRAK, *J. Thermophys.* **4** (1990) 79.